Single Molecule Electrochemical Detection in Aqueous Solutions and Ionic Liquids

ARTICLE *in* ANALYTICAL CHEMISTRY · SEPTEMBER 2015

Impact Factor: 5.64 · DOI: 10.1021/acs.analchem.5b02569

analytical chemistry

Article

pubs.acs.org/ac

Single Molecule Electrochemical Detection in Aqueous Solutions and Ionic Liquids

Joshua C. Byers, Binoy Paulose Nadappuram, David Perry, Kim McKelvey, Alex W. Colburn, and Patrick R. Unwin*

Department of Chemistry, University of Warwick, Coventry CV4 7AL, U.K.

Supporting Information

ABSTRACT: Single molecule electrochemical detection (SMED) is an extremely challenging aspect of electroanalytical chemistry, requiring unconventional electrochemical cells and measurements. Here, SMED is reported using a "quad-probe" (four-channel probe) pipet cell, fabricated by depositing carbon pyrolytically into two diagonally opposite barrels of a laser-pulled quartz quadruple-barreled pipet and filling the open channels with electrolyte solution, and quasi-reference counter electrodes. A meniscus forms at the end of the probe covering the two working electrodes and is brought into contact with a substrate working electrode surface. In this way, a nanogap cell is produced whereby the two carbon electrodes in the pipet can be used to promote redox cycling of an individual molecule with the substrate. Anticorrelated currents generated at the substrate and tip electrodes, at particular distances (typically tens of nanometers), are consistent with the detection of single molecules. The low background noise realized in this droplet format opens up new opportunities in single molecule electrochemistry, including the use of ionic liquids, as well as aqueous solution, and the quantitative assessment and analysis of factors influencing redox cycling currents, due to a precisely known gap size.

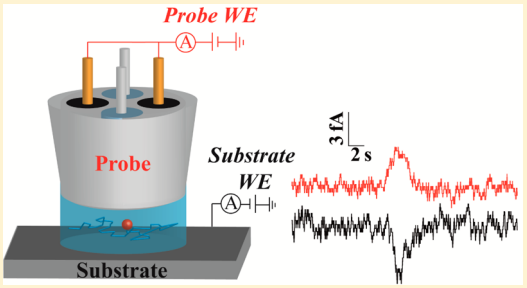

The detection and investigation of a single molecule diffusing freely in solution is at the forefront of emerging electrochemical and optical analytical detection techniques.[1,2] However, while optical methods have evolved into spectroscopic techniques,[3] electrochemical methods on the other hand have remained much more limited. A major challenge in these systems is the spatial localization of a single molecule for sufficient time to permit interrogation.[4] Single molecule electrochemical detection (SMED) offers significant opportunity for fundamental studies of homogeneous and heterogeneous charge transfer, with implications for sensing, energy conversion and storage, and biological processes. Yet, with few methods available for isolating an individual molecule and measuring charge transfer at an electrode, the number of examples of SMED is small despite two decades of effort.[1,5−8]

To measure the electrochemical current produced by an individual molecule, it is necessary to amplify the signal through redox cycling.[5] In this process, a single redox active molecule is isolated between two closely spaced electrodes (several tens of nanometers or less) where one electrode is held at an oxidizing potential and the other at a reducing potential with respect to a redox couple of interest. The same single molecule moves rapidly back and forth between the two electrodes undergoing tens of thousands (or more) of charge transfer events per second, thereby generating a tiny, but measurable, current. Initial demonstrations of SMED used a tip ultramicroelectrode (UME) that was held at a potential to oxidize a probe molecule and positioned close (estimated to be ∼10 nm) to a substrate electrode using a scanning electrochemical microscopy (SECM) format. The substrate was held at a reducing potential to promote redox cycling between the tip and substrate electrodes.[5] Intermittent peaks in electrochemical current at the tip were attributed to an individual molecule that became temporarily located, and shuttled, between the UME and substrate electrodes. In this configuration, measurements were limited to the tip electrode as the background noise level was too large to measure the redox cycling current at the substrate working electrode. These measurements were recognized to be extremely challenging,[9] and more recently, Lemay and coworkers[1,8] used a microfabricated thin layer cell, which contained two high surface area electrodes separated by a fixed distance, typically 40−70 nm, through which dilute solutions of a redox mediator were flowed, allowing for the detection of individual molecules, or small groups of molecules, as they occasionally entered into the cell and underwent redox cycling. A significant attribute of these latter studies was that the electrochemical current was measured separately at each electrode. This allowed for the measurement of the anticorrelated current (oxidation and reduction) at each electrode, confirming the occurrence of redox cycling of a single molecule. For this experimental arrangement it was found that adsorption of the probe molecule at the electrodes

Received: July 8, 2015
Accepted: September 23, 2015
Published: September 23, 2015

DOI: 10.1021/acs.analchem.5b02569
Anal. Chem. 2015, 87, 10450−10456

played a significant role and dramatically reduced the expected redox cycling efficiency, demonstrating that single molecule measurements could also act as local probes of their environment. However, these electrochemical cells are nontrivial to fabricate and use, and to date, single molecule measurements have relied exclusively on the use of noble metals such as Pt or Au as working electrodes and solvents where the diffusion coefficient is high.[1,5−8]

In this work, we use a simple new cell design for SMED that employs an easily prepared four channel micropipet, referred to as a "quad-probe"[10] that is approximately 3 μm in total diameter and used to form a droplet electrochemical cell that can be brought into contact with any working electrode substrate, greatly expanding the range of SMED systems that can be explored. The individual channels within the quad-probe were approximately 1 μm or less in size, depending on the overall probe diameter. Two of the four channels were filled with electrolyte solution and Ag/AgCl quasi-reference counter electrodes (QRCEs). The other two channels were filled with pyrolyzed carbon[11−13] to create two further working microelectrodes that could be used to promote redox cycling with a substrate working electrode (Figure 1a). The low surface area

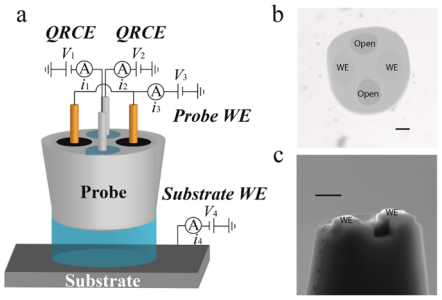

Figure 1. (a) Schematic of the electrode configuration: the carbon working electrodes in the barrel of the probe; two open barrels filled with electrolyte and AgCl-coated Ag wire QRCEs; and the substrate working electrode. The potentials of the two QRCEs (V_1 and V_2) were controlled using a custom potentiostat, while the potential at the tip and substrate working electrodes was controlled separately (V_3 and V_4) using independent electrometers. (b) SEM image (plan view) of a flat quad-probe, containing two carbon-filled and two open channels that was milled with a focused ion beam. (c) SEM images of quad-probes where quartz was preferentially milled away to reveal protruding carbon electrodes. Scale bar in (b) and (c) is 500 nm.

of the carbon microelectrodes greatly enhances the electrochemical signal-to-noise ratio. By further confining the volume of our measurements to a droplet formed at the end of the pipet we achieve *low noise levels* of only a few fA at each of the working electrodes. This makes possible the correlation of the electrochemical current generated at the tip and substrate and allows for the creation of nanogap electrochemical cells with *highly controllable* and *variable height* that can be used to trap and detect individual molecules. As a consequence of the exceptionally low noise levels achieved herein, we show the ability to detect and analyze the redox cycling of an individual molecule in a viscous ionic liquid, opening up new prospects in SMED.

EXPERIMENTAL SECTION

Materials and Reagents. (Ferrocenylmethyl)trimethylammonium ($FcTMA^+$) hexafluorophosphate was prepared in house from the metathesis of ferrocenyltrimethylammonium iodide (Strem Chemicals) and silver hexafluorophosphate (Strem Chemicals).[14] Phosphate buffer solution (PBS) (pH 7.2, Sigma-Aldrich), potassium chloride (AR grade, Sigma-Aldrich), hexaammineruthenium(III) ($Ru(NH_3)_6^{3+}$) chloride (98%, Acros Organics), and 1-butyl-3-methylimidazolium tetrafluoroborate [BMIM][BF_4] (HPLC grade, Sigma-Aldrich) were used as received. Multibore quartz quadruple-barreled capillaries (30 cm length, 1.57 mm outer diameter, 0.381 mm inner diameter) were cut into four equal length parts (MBT-015-062-4Q, Friedrich & Dimmock, Inc.).

Quad Probe Fabrication. Two types of quad probe electrodes were used in this work including a quad-barrel probe with coplanar carbon electrodes (Figure 1b) and a modified probe where the carbon electrodes protruded slightly from the end of the pipet (Figure 1c). A quartz quadruple-barreled capillary was pulled to a small tip diameter (~2−3 μm) using a laser puller (P-2000, Sutter Instruments) to produce a quad-probe with four open barrels that were each approximately 1 μm across. Two of the four barrels (diagonally opposed) of the pulled pipet were filled with pyrolytic carbon using butane gas as a carbon source.[10−13] Gallium ions (Ga^+) were used to mill the end of the pipet by a focused ion beam (FIB) (JEOL 4500, JEOL), resulting in two electrodes, that could be used for single molecule redox cycling with the substrate electrode. Focused ion beam milling could also be used to control the extent of carbon protrusion at the ends of the quad-probe tips, as it was found that quartz was removed at a faster rate than carbon, allowing for the formation of probes where carbon protruded from the ends (Figure 1c).

Nanogap Electrochemical Cell. A four electrode configuration (Figure 1a) was used comprising a tip working electrode formed by connecting the two carbon electrodes in series (copper wire) and measuring the total current at them. This was done to increase the overall electrode area for detection of the electrochemical current generated by redox cycling, but in future work these electrodes could be individually addressable.[10] The two open barrels were filled with a solution of interest along with two QRCEs (either Ag/AgCl or Ag wire). A small offset potential (typically 20−100 mV) was applied between the QRCEs, using a custom-built potentiostat. The potential between the two QRCEs in the barrels (V_1 and V_2) was controlled using a custom-built potentiostat. The resulting ion current was used as a feedback signal,[15,16] to detect meniscus contact with the working electrode substrate surface. The working electrode substrate surface was either an SPI-1 grade HOPG substrate (SPI supplies) or a Pt-coated glass slide. The potentials at the tip and substrate electrodes were precisely controlled via V_3 and V_4, as well as V_1 and V_2 (Figure 1a), and the working electrode currents (i_3 and i_4 in Figure 1a) were measured independently using custom-built electrometers.

To bring the tip and the substrate into meniscus contact, the tip position was oscillated sinusoidally in the normal direction (80 nm peak-to-peak, 288 Hz), as the tip was translated toward the substrate, and an ac ion current based feedback control scheme was used.[15,16] Once meniscus contact was achieved, the ac oscillation and dc offset potential were switched off, as the tip continued to be slowly approached to the substrate until contact or until a desired distance, was achieved, so that the gap dimensions were known with high accuracy.

An FPGA card (PCIe-7852R, National Instruments) with 16 bit analog input resolution was used for instrument control and data acquisition through a Labview interface. Fine positioning

DOI: 10.1021/acs.analchem.5b02569
Anal. Chem. 2015, 87, 10450−10456

of the pipet perpendicular to the surface utilized an LISA linear actuator (P-753.1CD, PI) and controller (E665, PI) with a 15 μm extended travel providing a step resolution of 0.46 nm. The faraday cage in which the apparatus was placed contained vacuum insulated panels (Kevothermal) and aluminum heat sinks (Hamilton Sundstrand) for thermal insulation to minimize any drift of the z-piezo position.[17] Further details of the experimental setup are given in the Supporting Information (SI), Sections S1–S2.

RESULTS AND DISCUSSION

Figure 2 shows the evolution of the tip and substrate current (electrode potential of 0.000 V vs Ag wire QRCE) as a pipet

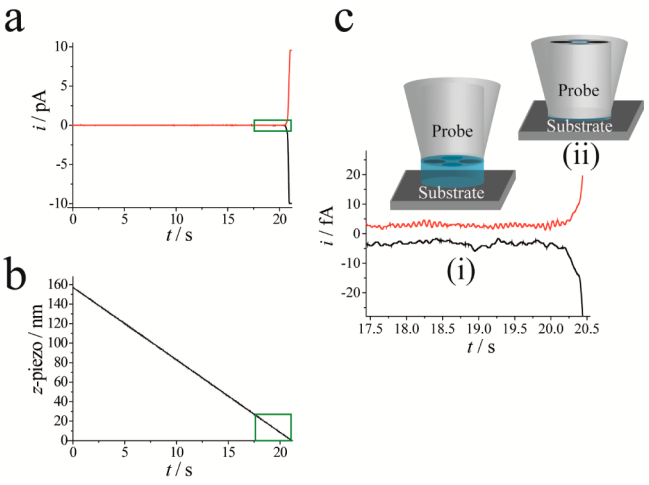

Figure 2. Approach curves for simultaneously acquired (a) tip (red line)/substrate (black line) current and (b) z-piezo position as a function of time. Approach rate was 7.5 nm s^{-1}. The probe (working electrode potential of +0.500 vs Ag wire QRCE) containing a blank [BMIM][BF_4] ionic liquid solvent was approached toward the Pt substrate until a sharp rise in current was observed following physical contact of the tip and substrate (electrode potential of 0.000 vs Ag wire QRCE). A z-piezo position of zero is defined by the onset of physical contact between the probe and substrate. (c) A zoom-in, highlighted by a green box in (a) and (b), illustrating the nanogap geometry formed (region (i)) for tip–substrate separations less than 30 nm and up until physical contact between the probe and substrate (region (ii)). For the blank [BMIM][BF_4] the currents were uncorrelated and showed a low background noise of ca. 1 fA.

(working electrode potential of +0.500 V vs Ag wire QRCE) containing a blank [BMIM][BF_4] ionic liquid solvent approached the surface after meniscus contact. The pipet probe was initially located ca. 150 nm from the Pt substrate electrode and approached the substrate at a constant velocity (7.5 nm s^{-1}) until a large jump in current was observed, corresponding to physical contact (short-circuit) between the probe and substrate. The simultaneously recorded tip/substrate currents (Figure 2a) and z-piezo position (Figure 2b) are both plotted as a function of time. A z-piezo position of zero is defined by the onset of physical contact between the probe and substrate. Knowledge of the exact position of tip–substrate contact was used to determine with high accuracy the interelectrode separation distance for single molecule events. Figure 2c shows a zoom-in of the tip and substrate currents (Figure 2a) for a separation of less than 30 nm. The currents show extremely small background noise levels (ca. 1 fA) which are not correlated in time up until the onset of physical contact.

The baseline noise level (~1 fA) represents an order of magnitude improvement compared to state-of-the-art microfabricated devices[1,8] (~10 fA) and a 2 orders of magnitude improvement compared to SECM[5−7] (hundreds of fA). As a consequence of the small background noise, for regions very close to the substrate (less than 50 nm from contact), and using probes filled with sufficiently dilute concentrations of a redox couple, it was possible to detect the anticorrelated currents due to redox cycling of an individual molecule as shown further below.

SMED was realized separately in aqueous solution and in an ionic liquid solvent. The redox probe molecule used in aqueous solution was $Ru(NH_3)_6^{3+}$, which undergoes a simple one electron reduction. The supporting electrolyte was 25 mM KCl in 50 mM PBS. The HOPG substrate was used to generate $Ru(NH_3)_6^{2+}$ by holding the potential at a value (−0.450 V vs Ag/AgCl QRCE) that corresponded to the limiting current of $Ru(NH_3)_6^{3+}$ reduction, while the tip was held at 0.000 V and used for collection (oxidation of $Ru(NH_3)_6^{2+}$ to $Ru(NH_3)_6^{3+}$). Figure 3 shows the results of two different approaches that were

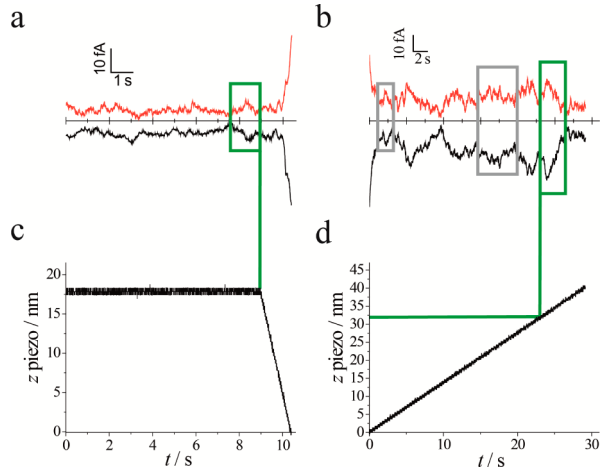

Figure 3. Single molecule measurements for a 10 nM aqueous solution of $Ru(NH_3)_6^{3+}$ in 50 mM phosphate buffer solution and 25 mM KCl. The upper panels display the current, and the lower panels display the corresponding z piezo position plotted as a function of time. The HOPG substrate was held at a reducing potential of −0.450 V (vs Ag/AgCl QRCE), and the tip electrode was held at 0.000 V (vs Ag/AgCl QRCE) and used for oxidation. (a) The redox cycling of a $Ru(NH_3)_6^{3+/2+}$ molecule can be seen ca. 18 nm away from the tip–substrate contact point (highlighted in green dashed box) while the z piezo position was constant. Following the redox cycling event, the tip was approached toward the substrate (translation rate 12.5 nm s^{-1}) until contact to determine the exact tip–substrate separation. (b) Anticorrelated current spikes were observed at both the substrate and tip (gray and green dashed boxes) with maximal current values of ca. 30 fA as the tip was retracted from the substrate surface at a constant velocity (translation rate 1.25 nm s^{-1}).

used to detect an individual molecule. In the first case (Figure 3a), the probe was held at a known fixed distance (18 nm) above the substrate until redox cycling was detected at the tip and substrate electrodes. In the second case (Figure 3b), redox cycling was observed after the tip was brought into contact with the substrate and then continuously retracted while a molecule was trapped within the droplet. In the upper panel of Figure 3, the current is plotted as a function of time while the z piezo position is plotted over the same period of time in the lower panel. A z piezo position of zero corresponds to initial tip–

DOI: 10.1021/acs.analchem.5b02569
Anal. Chem. 2015, 87, 10450−10456

substrate contact as defined by the point where the current at both electrodes saturates and corresponds to the onset of their physical contact (Figure 2).

In Figure 3a, the solution in the probe contained 10 nM $Ru(NH_3)_6^{3+}$ in 25 mM KCl and PBS. The average number of molecules, $\langle N \rangle$, expected for an 18 nm tip−substrate separation would be $\langle 0.76 \rangle$ leading to stochastic fluctuations in the measured electrochemical current.[4,18] Evidently a single molecule enters into the droplet at ca. 7 s. Up until this time, the measured current, which showed small fluctuations, was uncorrelated. However, at times longer than 7 s, the tip and substrate display anticorrelated currents, with the substrate (−0.450 V vs Ag/AgCl QRCE) showing transient increases in cathodic current and the tip (+ 0.000 V vs Ag/AgCl QRCE) showing corresponding increases in the anodic current that are anticorrelated in magnitude and time, consistent with redox cycling.[1,8] Following the detection of this event, the tip was approached toward the substrate (approach rate 12.5 nm s^{-1}) and stopped as soon as tip−substrate contact was detected to determine precisely the exact tip−substrate separation for the single molecule event highlighted. Subsequently, the tip was retracted (retract rate 1.25 nm s^{-1}) from the substrate. A faster translation rate was used for the approach to shorten the time between the observation of a single molecule event and tip−substrate contact in order to minimize any contributions from thermal drift. During retraction, a slower translation rate, but one that exceeded that of thermal drift, was used because the tip−substrate separation had already been determined. The corresponding current transients are shown in Figure 3b as the tip moved away from the substrate at a constant velocity. Again, the current shows anticorrelated behavior with several distinct peaks observed whose duration was much longer than the time constant of the electrometer (100 ms). These features can be attributed to the cycling of an individual molecule between the tip and substrate with a few events occurring for a sufficient time to be clearly resolved, as highlighted by the green box in Figure 3b. The duration of this current enhancement was approximately 1 s, during which the current peaked and plateaued with a magnitude of ca. 30 fA, compared to the baseline at larger tip−substrate separations.

For a 30 nm tip−substrate separation, we would have expected to observe 146 fA per molecule (assuming the current $i_{redox} = eD/z^2$ where e is the charge of an electron, D is the diffusion coefficient, which is 8.2×10^{-6} cm^2 s^{-1} for $Ru(NH_3)_6^{3+/2+}$ in water,[19] and z is the tip−substrate separation). We do not consider a contribution from convection, as previous measurements using SECCM have shown that droplet evaporation does not noticeably impact mass transport rates.[20] The reduced magnitude of the measured currents for single molecule redox cycling has been previously attributed to adsorption of the molecule at the electrodes.[21,22] This may play a role in these studies. However, for the studies herein, we also have to consider inactive regions across the tip surface, as discussed further below. For such small current measurements the electrometer response function also attenuates the signal (see SI, Section S3). Overall, the measured current values are consistent with recent reports of single molecule cycling in a nanogap thin layer cell where a comparable diminution in current magnitude was observed in aqueous conditions.[1]

For tip−substrate separations of less than 40 nm many sharp distinct anticorrelated events can be resolved (Figure 3d), which, due to the low background noise level (~few fA) obtainable in this configuration, provides an order of magnitude better signal-to-noise ratio compared with previous measurements.[1,5−8] Several events are highlighted in Figure 3b with gray and green dashed boxes. Events highlighted in gray boxes correspond to cases where the molecule rapidly cycles between the two active electrodes for short periods of time before leaving the active region briefly and then returning due to the random walk of the molecule in the meniscus droplet. While the HOPG substrate is uniformly active, the tip contains some areas where cycling does not occur such as the glass outer diameter and inner septum as well as the open barrels (Figure 4a). A three-dimensional random walk simulation (Figure 4) was used to map the movement of a molecule confined within a closed system[23] (i.e., the molecule could not escape up the open barrels) within the droplet that takes into account a reduced active area at the probe. For the simulation, the substrate was assumed to be uniformly active while only the carbon UMEs were assumed to be active for the probe end (Figure 4a). A charge transfer event occurred for each instance that an oxidized molecule reached the substrate working electrode boundary, and similarly, a charge transfer event occurred each time a reduced molecule contacted the active area of one of the carbon UMEs. Further details of the simulation, including simulation parameters and the attenuation of the current magnitude due to the response of the electrometer,[4] are available in the SI, Section S3. Figure 4c illustrates the electrochemical current generated by a single molecule trapped within the droplet over a 1 s time period whose profile has been modulated by the electrometer response time (see SI, Section S3). At time $t = 0$, a single molecule is located directly in the center of the droplet (Figure 4b), which then undergoes a random walk for a period of 1 s. Figure 4c shows the evolution of the electrochemical current, where initially it was zero at time $t = 0$ (molecule located in the center of the droplet) and then increases as the molecule undergoes a random walk throughout the droplet volume. It can be seen that many brief events occur that are much shorter than the time constant of the electrometer (100 ms), which leads to

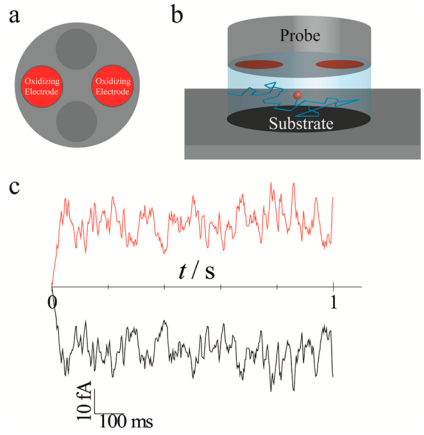

Figure 4. (a) 2D schematic of the probe electrode illustrating the active oxidizing electrode (red) and inactive (gray) areas. (b) 3D geometry for the random walk simulation where a single molecule was positioned in the center of the droplet at $t = 0$. Red areas (probe) correspond to the oxidizing electrode, and the black area (substrate) corresponds to the reducing electrode. (C) Current transients based on 3D random walk simulation for a tip−substrate separation of 30 nm.

DOI: 10.1021/acs.analchem.5b02569
Anal. Chem. 2015, 87, 10450−10456

sharp peaks and variations in current that do not reach the theoretical maximum current for uniformly active electrodes (146 fA for z = 30 nm). Significantly, the associated anticorrelated current profiles and magnitudes (Figure 4c), which show fluctuations with time as the molecule samples the entire droplet volume, resemble the experimental current transients measured in Figure 3.

Single molecule measurements in an ionic liquid have not yet been possible due to the exceptionally low diffusion coefficients realized in such relatively viscous media,[24−26] resulting in current magnitudes that would be too small to be clearly resolved by previous techniques. Using our configuration it was possible to achieve background noise levels of a femtoampere or less (Figure 2c) allowing us to detect events with a current magnitude of only a few femtoamperes. Measurements were carried out using the ionic liquid [BMIM][BF_4], 100 nM $FcTMA^+$ as a redox probe, and a quad-probe containing protruding carbon working electrodes (Figure 1c). The tip working electrode was held at an oxidizing potential (+ 0.500 V vs Ag wire QRCE) to generate $FcTMA^{2+}$ and approached a Pt substrate that was held at a reducing potential for collection (0.000 V vs Ag wire QRCE). For these measurements the tip was brought into contact with the substrate, withdrawn 10 nm from the surface, and then held at a fixed distance while the tip and substrate currents were recorded. Figure 5a shows current

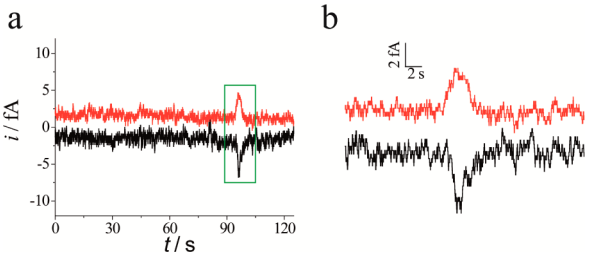

Figure 5. (a) Current−time plot for a solution containing 100 nm $FcTMA^+$ in [BMIM][BF_4] at a constant z piezo position. A redox cycling event highlighted by the green box is shown as a zoom-in (b). The tip electrode was held at +0.500 V (vs Ag wire QRCE) to generate $FcTMA^{2+}$, and a Pt substrate was held at a reducing potential of 0.000 V (vs Ag wire QRCE) to regenerate $FcTMA^+$.

time plots for the tip and substrate working electrodes over a period of several minutes. These data highlight the very stable and low background currents that prevail over extended periods. A redox cycling event is highlighted by a green box (Figure 5a) with a zoom-in shown in Figure 5b. At the end of the measurement (within 60 s of the single molecule event), the tip−substrate separation for the highlighted single molecule event (34 nm) was determined by approaching the tip toward the substrate until physical contact was made. Scanning electron microscope images of the probe along with the corresponding footprint created on the substrate due to probe contact are shown in Figure 6a and 6b. The droplet size on the substrate can be assumed to correspond to the size of the footprint during measurement as the low vapor pressure of the ionic liquid at atmospheric pressure and under vacuum (SEM) lead to negligible solvent evaporation.[27,28] The outline of the probe (Figure 6a) and droplet (Figure 6b) are similar in size and shape with the droplet showing slightly increased dimensions due to a combination of surface wetting and solution spreading as the probe was brought into contact with the substrate. Overall, the droplet size reflects closely that of the

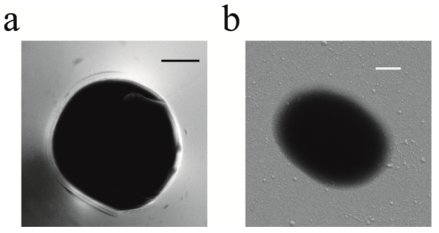

Figure 6. Plan-view SEM image of (a) probe used for single molecule measurements in Figure 5 and (b) corresponding footprint left behind by [BMIM][BF_4] ionic liquid on the Pt substrate. Scale bar is 1 μm in (a) and (b).

probe, highlighting the well-defined geometry realized using this method.

The peak currents at both the tip and substrate working electrodes (∼4 fA) could be clearly resolved from the background current (∼1 fA) allowing us to detect the redox cycling of a single molecule ($FcTMA^+/FcTMA^{2+}$) in an ionic liquid. The diffusion coefficient of $FcTMA^+$ was measured using a 25 μm diameter Pt UME in bulk solution and found to be 8×10^{-8} cm^2 s^{-1} (SI, Section S4). In this case, a peak current of 1.1 fA would have been expected for a single molecule randomly diffusing between two electrodes for a tip−substrate separation of 34 nm. The higher current value would suggest that the simple description based on diffusion in a thin layer cell, free from migration, may not fully account for the expected electrochemical current in an ionic liquid for such a confined geometry. Considerable discussion[29−32] has centered around the extent of ion dissociation in ionic liquids following a recent assertion that they should be considered as dilute electrolytes[33] resulting in a diffuse layer that could extend out to 10 nm or more from the electrode/IL interface. The resulting electric field across the nanogap would result in a larger than expected limiting current due to the small electrode spacing.[34] In fact, it has been shown in aqueous solution that redox cycling without a supporting electrolyte can lead to a 2000-fold enhancement of the limiting current as a result of migration due to the electric field between the generator and collector electrodes.[35] The results herein highlight a significant, but more moderate, effect and suggest a diffuse layer effect that impacts mass transport in the nanogap geometry. Considering the large overall electric field that would exist across the gap in the absence of the supporting electrolyte (∼15 kV cm^{-1}), a diffuse layer that extends only a few nanometers from the surface could have a significant impact in such a confined geometry, making it quite reasonable to expect migration to play a role in this configuration and contribute to the enhanced current observed here.

■ CONCLUSIONS AND OUTLOOK

The detection of single molecules in aqueous and ionic liquid solvents has been demonstrated using a droplet based approach. A significant advantage of this method is the ability to characterize the tip−substrate separation and electrode area directly, instead of relying on the redox electrochemical signal itself, which may provide only an indirect estimate of these parameters. The currents generated during SMED were supported by a random walk simulation (3D), which indicates that the molecule rapidly explores the entire volume of the droplet. Single molecule measurements, to date, have been carried out using an electrode potential corresponding to the limiting current to maximize signal generation as also used

DOI: 10.1021/acs.analchem.5b02569
Anal. Chem. 2015, 87, 10450−10456

herein. In the future, by increasing the probe electrode area in combination with the high sensitivity capability realized here, potential dependent measurements could become possible. Moreover, in an alternative configuration where the carbon probe electrodes are not shorted together, but the electrodes are independently addressable, it would become possible to measure the spatial location of a molecule in addition to redox cycling. It is further important to point out that the carbon pipet electrodes can be readily functionalized via a variety of methods.[10,12,13,36−39]

There are several more opportunities that could be explored further using the setup for SMED demonstrated here. For example, the ion flux through the electrolyte-filled barrels, which is dependent on the dc bias applied across them,[20,40] can be used to control the flux of charged species within the droplet meniscus and effect the frequency of events occurring similarly to a microfluidic configuration where the flow rate can be used for this purpose.[4] Most importantly, the ability to control the tip−substrate distance and measure the anticorrelated currents between the tip and substrate, as a function of tip−substrate separation, offers new opportunities for fundamental studies of the redox cycling of individual molecules under a variety of conditions and at different substrates, as the probe can be used to approach essentially any surface. Given the exceptionally low noise (∼1 fA) combined with the ability to create extremely small gaps this probe electrode configuration should allow the influence of the double layer between two closely spaced electrodes to be investigated, where distance-dependent solvent structure effects may be manifested as revealed using ionic liquids. For these systems it has been found that mass transport perpendicular to the electrodes is enhanced by electric field effects. This opens up opportunities for fundamental studies of this type using the approach outlined here.

■ ASSOCIATED CONTENT

Supporting Information

The Supporting Information is available free of charge on the ACS Publications website at DOI: 10.1021/acs.analchem.5b02569.

Further details of the experimental setup, drift measurements, random walk simulation details, diffusion coefficient measurement, and electrode roughness (PDF)

■ AUTHOR INFORMATION

Corresponding Author

*E-mail: p.r.unwin@warwick.ac.uk.

Notes

The authors declare no competing financial interest.

■ ACKNOWLEDGMENTS

We thank the European Research Council (ERC-2009-AdG247143-QUANTIF) together with the University of Warwick (CS studentship for B.P.N.) for support. The research leading to these results has received funding from the European Union Seventh Framework Programme (FP7/2007-2013) under Grant Agreement No. 329953. We thank Prof. Shigeru Amemiya (Department of Chemistry, University of Pittsburgh, USA) for helpful advice on isothermal insulation of the faraday cage used here, Dr. Yangrae Kim for assistance with picomotor installation and calibration, and Dr. Robert Lazenby and Ms. Minkyung Kang for acquiring TEM images.

■ REFERENCES

(1) Kang, S.; Nieuwenhuis, A. F.; Mathwig, K.; Mampallil, D.; Lemay, S. G. *ACS Nano* **2013**, *7*, 10931.
(2) Schlau-Cohen, G. S.; Bockenhauer, S.; Wang, Q.; Moerner, W. E. *Chem. Sci.* **2014**, *5*, 2933.
(3) Lord, S. J.; Lee, H. D.; Moerner, W. E. *Anal. Chem.* **2010**, *82*, 2192.
(4) Singh, P. S.; Kätelhön, E.; Mathwig, K.; Wolfrum, B.; Lemay, S. G. *ACS Nano* **2012**, *6*, 9662.
(5) Fan, F.-R. F.; Bard, A. J. *Science* **1995**, *267*, 871.
(6) Fan, F.-R. F.; Kwak, J.; Bard, A. J. *J. Am. Chem. Soc.* **1996**, *118*, 9669.
(7) Sun, P.; Mirkin, M. V. *J. Am. Chem. Soc.* **2008**, *130*, 8241.
(8) Zevenbergen, M. A. G.; Singh, P. S.; Goluch, E. D.; Wolfrum, B. L.; Lemay, S. G. *Nano Lett.* **2011**, *11*, 2881.
(9) Lemay, S. G.; Kang, S.; Mathwig, K.; Singh, P. S. *Acc. Chem. Res.* **2013**, *46*, 369.
(10) Paulose Nadappuram, B.; McKelvey, K.; Byers, J. C.; Güell, A. G.; Colburn, A. W.; Lazenby, R. A.; Unwin, P. R. *Anal. Chem.* **2015**, *87*, 3566.
(11) Takahashi, Y.; Shevchuk, A. I.; Novak, P.; Zhang, Y.; Ebejer, N.; Macpherson, J. V.; Unwin, P. R.; Pollard, A. J.; Roy, D.; Clifford, C. A.; Shiku, H.; Matsue, T.; Klenerman, D.; Korchev, Y. E. *Angew. Chem., Int. Ed.* **2011**, *50*, 9638.
(12) McKelvey, K.; Nadappuram, B. P.; Actis, P.; Takahashi, Y.; Korchev, Y. E.; Matsue, T.; Robinson, C.; Unwin, P. R. *Anal. Chem.* **2013**, *85*, 7519.
(13) Nadappuram, B. P.; McKelvey, K.; Al Botros, R.; Colburn, A. W.; Unwin, P. R. *Anal. Chem.* **2013**, *85*, 8070.
(14) Bertoncello, P.; Ciani, I.; Li, F.; Unwin, P. R. *Langmuir* **2006**, *22*, 10380.
(15) Ebejer, N.; Schnippering, M.; Colburn, A. W.; Edwards, M. A.; Unwin, P. R. *Anal. Chem.* **2010**, *82*, 9141.
(16) Ebejer, N.; Güell, A. G.; Lai, S. C. S.; McKelvey, K.; Snowden, M. E.; Unwin, P. R. *Annu. Rev. Anal. Chem.* **2013**, *6*, 329.
(17) Kim, J.; Shen, M.; Nioradze, N.; Amemiya, S. *Anal. Chem.* **2012**, *84*, 3489.
(18) Bard, A. J.; Fan, F.-R. F. *Acc. Chem. Res.* **1996**, *29*, 572.
(19) Güell, A. G.; Ebejer, N.; Snowden, M. E.; McKelvey, K.; Macpherson, J. V.; Unwin, P. R. *Proc. Natl. Acad. Sci. U. S. A.* **2012**, *109*, 11487.
(20) Snowden, M. E.; Güell, A. G.; Lai, S. C. S.; McKelvey, K.; Ebejer, N.; O'Connell, M. A.; Colburn, A. W.; Unwin, P. R. *Anal. Chem.* **2012**, *84*, 2483.
(21) Kätelhön, E.; Krause, K. J.; Mathwig, K.; Lemay, S. G.; Wolfrum, B. *ACS Nano* **2014**, *8*, 4924.
(22) Mampallil, D.; Mathwig, K.; Kang, S.; Lemay, S. G. *J. Phys. Chem. Lett.* **2014**, *5*, 636.
(23) Feldberg, S. W.; Edwards, M. A. *Anal. Chem.* **2015**, *87*, 3778.
(24) Carano, M.; Bond, A. M. *Aust. J. Chem.* **2007**, *60*, 29.
(25) Walsh, D. A.; Lovelock, K. R. J.; Licence, P. *Chem. Soc. Rev.* **2010**, *39*, 4185.
(26) Lovelock, K. R. J.; Cowling, F. N.; Taylor, A. W.; Licence, P.; Walsh, D. A. *J. Phys. Chem. B* **2010**, *114*, 4442.
(27) Armstrong, J. P.; Hurst, C.; Jones, R. G.; Licence, P.; Lovelock, K. R. J.; Satterley, C. J.; Villar-Garcia, I. J. *Phys. Chem. Chem. Phys.* **2007**, *9*, 982.
(28) Arimoto, S.; Oyamatsu, D.; Torimoto, T.; Kuwabata, S. *ChemPhysChem* **2008**, *9*, 763.
(29) Perkin, S.; Salanne, M.; Madden, P.; Lynden-Bell, R. *Proc. Natl. Acad. Sci. U. S. A.* **2013**, *110*, E4121.
(30) Gebbie, M. A.; Valtiner, M.; Banquy, X.; Henderson, W. A.; Israelachvili, J. N. *Proc. Natl. Acad. Sci. U. S. A.* **2013**, *110*, E4122.
(31) Yochelis, A. *Phys. Chem. Chem. Phys.* **2014**, *16*, 2836.
(32) Lee, A. A.; Vella, D.; Perkin, S.; Goriely, A. *J. Phys. Chem. Lett.* **2015**, *6*, 159.
(33) Gebbie, M. A.; Valtiner, M.; Banquy, X.; Fox, E. T.; Henderson, W. A.; Israelachvili, J. N. *Proc. Natl. Acad. Sci. U. S. A.* **2013**, *110*, 9674.

DOI: 10.1021/acs.analchem.5b02569
Anal. Chem. 2015, 87, 10450−10456

(34) Gebbie, M. A.; Dobbs, H. A.; Valtiner, M.; Israelachvili, J. N. *Proc. Natl. Acad. Sci. U. S. A.* **2015**, *112*, 7432.
(35) Ma, C.; Contento, N. M.; Bohn, P. W. *J. Am. Chem. Soc.* **2014**, *136*, 7225.
(36) Actis, P.; Tokar, S.; Clausmeyer, J.; Babakinejad, B.; Mikhaleva, S.; Cornut, R.; Takahashi, Y.; López Córdoba, A.; Novak, P.; Shevchuck, A. I.; Dougan, J. A.; Kazarian, S. G.; Gorelkin, P. V.; Erofeev, A. S.; Yaminsky, I. V.; Unwin, P. R.; Schuhmann, W.; Klenerman, D.; Rusakov, D. A.; Sviderskaya, E. V.; Korchev, Y. E. *ACS Nano* **2014**, *8*, 875.
(37) Clausmeyer, J.; Actis, P.; López Córdoba, A.; Korchev, Y.; Schuhmann, W. *Electrochem. Commun.* **2014**, *40*, 28.
(38) Bélanger, D.; Pinson, J. *Chem. Soc. Rev.* **2011**, *40*, 3995.
(39) Kranz, C. *Analyst* **2014**, *139*, 336.
(40) O'Connell, M. A.; Snowden, M. E.; McKelvey, K.; Gayet, F.; Shirley, I.; Haddleton, D. M.; Unwin, P. R. *Langmuir* **2014**, *30*, 10011.

DOI: 10.1021/acs.analchem.5b02569
Anal. Chem. 2015, 87, 10450−10456